

Partial gap opening on the Fermi surface of the noncentrosymmetric superconductor $\text{Mo}_3\text{Al}_2\text{C}$ T. Koyama,^{1,*} Y. Ozaki,¹ K. Ueda,¹ T. Mito,¹ T. Kohara,¹ T. Waki,² Y. Tabata,² C. Michioka,³ K. Yoshimura,³ M.-T. Suzuki,⁴ and H. Nakamura²¹Graduate School of Material Science, University of Hyogo, Kamigori, Hyogo 678-1297, Japan²Department of Materials Science and Engineering, Kyoto University, Kyoto 606-8501, Japan³Department of Chemistry, Graduate School of Science, Kyoto University, Kyoto 606-8502, Japan⁴CCSE, Japan Atomic Energy Agency, 5-1-5, Kashiwanoha, Kashiwa, Chiba 277-8587, Japan

(Received 12 August 2011; revised manuscript received 19 October 2011; published 27 December 2011)

We report the results of ^{27}Al nuclear magnetic resonance and specific-heat measurements of the noncentrosymmetric superconductor $\text{Mo}_3\text{Al}_2\text{C}$ in the normal state. The phase transition at ~ 130 K is inferred from a distinct change in the NMR spectrum, a clear peak in the spin-echo decay rate, and an anomaly in the specific heat. At ~ 130 K, the Knight shift and the spin-lattice relaxation rate $1/T_1$ exhibit a significant decrease, which is associated with a reduction in the conduction electron density. These results suggest most probably charge-density wave ordering at ~ 130 K. Furthermore, the decrease in $1/T_1$ below the superconducting transition temperature suggests that superconductivity emerges on the partially quenched Fermi surface.

DOI: [10.1103/PhysRevB.84.212501](https://doi.org/10.1103/PhysRevB.84.212501)

PACS number(s): 74.70.Wz, 71.45.Lr, 74.25.nj, 71.27.+a

Another phase transition prior to the emergence of superconductivity (SC) has fostered research in the field of condensed-matter physics because the corresponding electronic states may enable us to understand the nature of SC in the ordered state. In recent years, the coexistence of ordered magnetism and SC in heavy-fermion superconductors has been studied extensively. The spin-density fluctuation plays an important role in imparting SC to these systems. In some frustrated magnets, spin-driven structural phase transition releases the spin frustration, and s -wave SC emerges at low temperatures.^{1,2} Thus the detail study of the normal-state properties is important and valuable.

A metallic carbide, $\text{Mo}_3\text{Al}_2\text{C}$, exhibits SC at $T_c = 9$ K.³ This compound has a β -Mn-type (space group $P4_132$) crystal structure, which does not possess a center of inversion. SC without spatial inversion symmetry has been extensively studied since the discovery of CePt_3Si in order to determine novel superconducting properties.⁴ Recently, Bauer *et al.* and Karki *et al.* independently investigated properties in the normal and superconducting states of polycrystalline samples of $\text{Mo}_3\text{Al}_2\text{C}$.^{5,6} This compound is a type-II superconductor that exhibits a specific-heat jump at T_c , $\Delta C_p/\gamma T_c \approx 2.2$, which is higher than the BCS value of 1.43. The upper critical field is close to the estimated paramagnetic limiting field. A notable feature of this compound is the power-law behavior of the specific heat and the nuclear spin-lattice relaxation rate $1/T_1$ in the superconducting state, which suggests that the order parameter is not of conventional s -wave SC. On the other hand, a measurement of the magnetic penetration depth suggested a conventional s -wave superconducting state.⁷ Thus the nature of SC in this compound is still controversial. In terms of normal-state properties, $\text{Mo}_3\text{Al}_2\text{C}$ is a weakly correlated electron system. The Sommerfeld value is estimated to be $\gamma \approx 18$ mJ/mol K². The magnetic susceptibility shows a temperature-independent Pauli paramagnetic behavior. According to band structure calculations, the states at E_F are derived almost entirely from the d bands of Mo.^{5,6}

In this Brief Report, we report the results of ^{27}Al nuclear magnetic resonance (NMR) and specific-heat measurements

of the superconducting carbide $\text{Mo}_3\text{Al}_2\text{C}$. The substantial change in the Fermi-level density of states, $D(E_F)$, at ~ 130 K is inferred from $1/T_1$ and the Knight shift. In addition, an appreciable anomaly in the specific heat is observed at 128 K. Therefore, we conclude that the partial gap opens on the Fermi surface at ~ 130 K. Furthermore, $1/T_1$ decreases below T_c , which clearly indicates that SC emerges at the residual density of the states at E_F in $\text{Mo}_3\text{Al}_2\text{C}$.

Polycrystalline samples of $\text{Mo}_3\text{Al}_2\text{C}$ were arc-melted under an argon atmosphere as described in detail elsewhere.⁶ The x-ray diffraction pattern shows that the samples contain minimal amounts of Mo_3Al_8 , MoC, and Mo as impurity phases. The temperature dependence of the specific heat was measured using a physical property measurement system (PPMS; Quantum Design). The NMR experiment was carried out using a conventional phase-coherent pulsed spectrometer. For the ^{27}Al NMR experiment, we also prepared a sample of Mo_3Al_8 , which is the most probable impurity phase containing Al nuclei, and measured it independently to confirm that Mo_3Al_8 does not show the phase transition at ~ 130 K.⁸ As a result, we are convinced that the observed phase transition at ~ 130 K is an intrinsic property of $\text{Mo}_3\text{Al}_2\text{C}$.

Figures 1(a) and 1(b) show typical ^{27}Al NMR line shapes measured by integrating the spin-echo intensity in a field-swept condition at a constant frequency of 83.5 MHz. The observed shape at 170 K is relatively sharp and symmetric, indicating that quadrupolar interaction is negligible at the Al position (8c site). This observation is consistent with a small electronic field gradient (EFG) observed at the 8c (Mn-I) site in β -Mn.⁹ We found that the line shape at 50 K differs from those at high temperatures. The line broadens and has additional broad components at the foot of the sharp line, as shown in Fig. 1(b). The dips at both sides of the central line are attributed to the superposition of the free induction decay (FID) signal from the sharp central line. The width of the broad components is independent of the magnetic field, indicating that this broadening is due to the appearance of satellite lines owing to the enhancement of the EFG at the Al position. To illustrate the temperature evolution of the sharp central

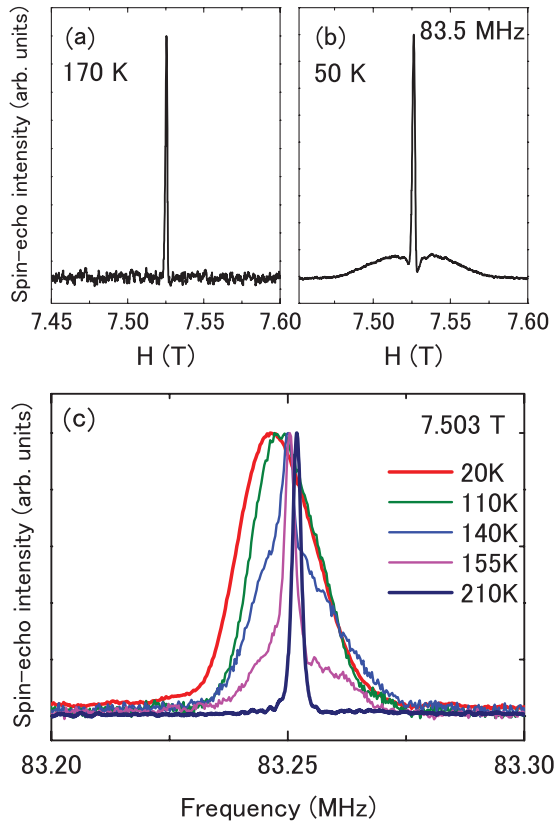


FIG. 1. (Color online) ^{27}Al NMR spectra obtained by sweeping the magnetic field at a fixed frequency at (a) 170 and (b) 50 K. The measurement condition was set appropriately to record broad components. (c) Temperature dependence of the central line of the ^{27}Al NMR spectrum. Data were obtained using a fast-Fourier-transform technique at a constant magnetic field to selectively observe the sharp line.

line, we show in Fig. 1(c) the NMR spectra obtained using a fast-Fourier-transform (FFT) technique at a constant magnetic field, $H = 7.503$ T. This technique is useful to observe the sharp NMR line. The line shape at 210 K is reproduced well by a symmetric Lorentzian function with a full width at half maximum (FWHM) of 3 kHz. The line changes its shape significantly as the temperature decrease from 160 to 120 K. A broad component appears at the bottom of the sharp line below 160 K and develops down to 120 K. The line attains a FWHM of 20 kHz below 100 K. Because the NMR spectra are sensitive to the environment of the observed nuclei, this result suggests an abrupt change in the electronic state, i.e., the phase transition at ~ 130 K.

Next, we carefully measured the specific heat, as shown in Fig. 2. An appreciable anomaly is observed at ~ 128 K, which is evidenced by a change in slope, as seen in the inset of Fig. 2. This observation supports the phase transition in the normal state.

Figure 3 shows the temperature dependence of the spin-echo decay rate $1/T_2$. The spin-echo decay curves do not follow the form of $\exp(-2\tau/T_2)$, where τ is the time separation between two $(\pi/2 - \pi)$ pulses. We tentatively estimate T_2 using double-exponential functions, $A_1 \exp(-2\tau/T_{2S}) + A_2 \exp(-2\tau/T_{2L})$, where A_1 and A_2 are adjustable parameters.

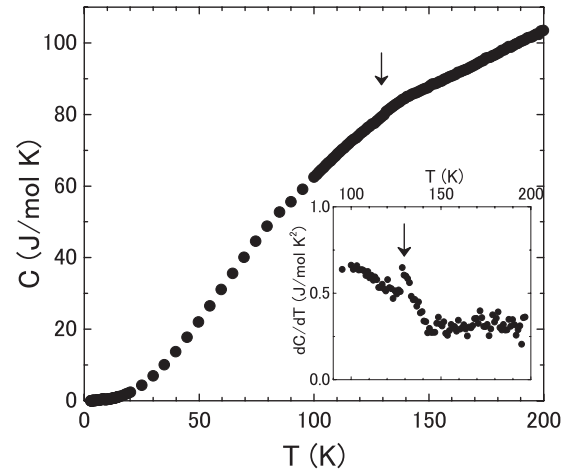


FIG. 2. Temperature dependence of the specific heat. The inset shows its temperature derivative. The arrows indicate a change in the slope at ~ 130 K.

The short component T_{2S} is expected to probe an intrinsic relaxation. On the other hand, the long component T_{2L} , which exhibits nearly temperature-independent behavior, may originate from impurities. The most remarkable result is the peak of $1/T_2$ at ~ 130 K, indicating the presence of an anomaly in the nuclear spin-spin coupling. This result is discussed later.

We measured $1/T_1$ using a radio-frequency (rf) comb-pulse saturation method. The nuclear magnetization of the sharp central line was selectively obtained by the recovery of the FID signal. When the linewidth $\Delta\omega$ is smaller than the amplitude of the rf field H_1 , i.e., $\Delta\omega/\gamma_n < H_1$, where γ_n is the gyromagnetic ratio, all the nuclear levels are easily saturated by the comb pulse. As a result, the recovery curve $m(t)$ of the nuclear magnetization $M(t)$ at time t after the saturation pulse, which is defined by $m(t) = [M(\infty) - M(t)]/M(\infty)$, should be of the single-exponential type. However, in spite of the sharp central line, $m(t)$ exhibits nonexponential behavior at all temperatures, which is characterized by the convex curve, as shown in the inset of Fig. 4. In order to extract $1/T_1$, we fitted the recovery curves to a stretched exponential function,

$$m(t) = \exp\left[-\left(\frac{t}{T_1}\right)^\beta\right], \quad (1)$$

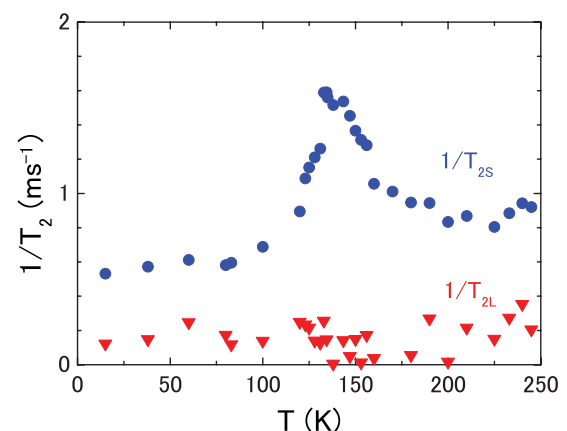


FIG. 3. (Color online) Temperature dependence of $1/T_2$.

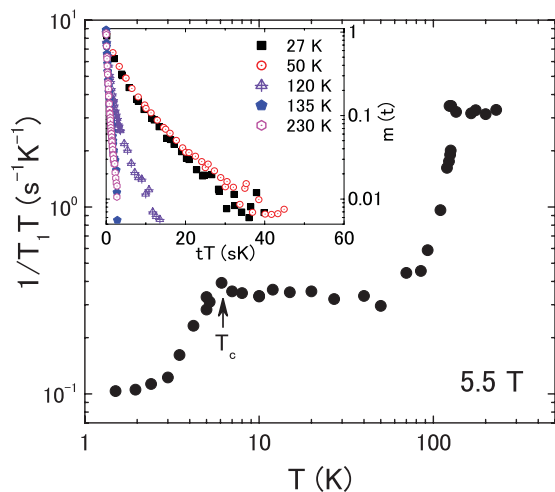


FIG. 4. (Color online) Temperature dependence of $1/(T_1T)$ at 5.5 T. T_1 values were derived using the stretched exponential function. The inset shows the nuclear recovery curve of the nuclear magnetization $m(t) = [M(\infty) - M(t)]/M(\infty)$ plotted against tT at several temperatures. Data were obtained by the recovery of the free induction decay signal.

where β is the stretching exponent, $0 < \beta \leq 1$.¹⁰ This relation is often observed when $1/T_1$ is inhomogeneously distributed owing to impurities and/or crystal imperfection. In the present case, the former is attributed mainly to the distribution of T_1 . The obtained β (~ 0.7) is nearly temperature independent above and below the transition temperature, indicating that the characteristic of $m(t)$ does not vary with temperature.

Figure 4 shows the temperature dependence of $1/(T_1T)$ at $H = 5.5$ T. As expected for a Pauli paramagnetic metal, the product T_1T becomes constant above 140 K. The most remarkable aspect of $1/(T_1T)$ is a rapid decrease in its magnitude at ~ 120 K. This indicates the possible existence of an energy gap at E_F . T_1T becomes constant below ~ 90 K, suggesting the presence of the residual density of states at E_F . The present $1/(T_1T)$ value below 90 K is four times larger than that reported previously.⁵ The discrepancy is ascribed to the different recovery function employed to extract $1/T_1$. The values of $1/(T_1T)$ at low temperatures are smaller than those at high temperatures by one order of magnitude. In general, temperature-independent $1/(T_1T)$ is roughly expressed as $1/(T_1T) \propto D(E_F)^2$. Using this relation, $D(E_F)$ is estimated to decrease by 70% at the transition. With further decrease in temperature, $1/(T_1T)$ decreases below T_c (~ 6.2 K at 5.5 T). This confirms that SC emerges on the small Fermi surface formed at the phase transition. Unfortunately, we cannot discuss the symmetry of the gap function using the $1/T_1$ data because in the superconducting state, the decrease in β as the temperature decrease below T_c makes the temperature dependence of $1/T_1$ ambiguous.

The sudden decrease in $D(E_F)$ is also inferred from the temperature dependence of the ^{27}Al Knight shift (^{27}K) shown in Fig. 5. ^{27}K is positive and much smaller than that of Al metal (0.16%) in whole temperature range. It shows a sudden drop at ~ 130 K. For elements without magnetic ions, the Knight shift K mainly consists of the Fermi-contact term K_s , the

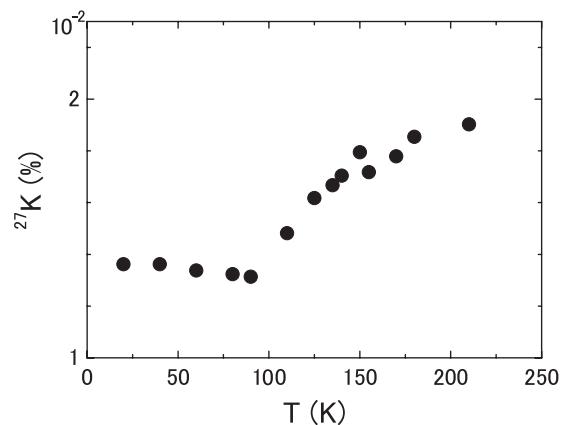


FIG. 5. Temperature dependence of the ^{27}Al Knight shift.

diamagnetic term K_{dia} , and the orbital term K_{orb} , and it can be expressed as

$$K = K_s + K_{\text{dia}} + K_{\text{orb}}. \quad (2)$$

Among these three terms, both K_s and K_{dia} are related to the Pauli paramagnetic susceptibility χ_P , namely $D(E_F)$. By assuming that K_{orb} is temperature independent, the drop in ^{27}K is ascribed to a decrease in $D(E_F)$. The origin of the weak temperature dependence of ^{27}K above ~ 130 K is not obvious but may be associated with the higher order temperature-dependent term in χ_P originating in the fine band structure near E_F .

We argue that the reduction in $1/(T_1T)$ and ^{27}K at the transition is connected with the appearance of a gap in $D(E_F)$ resulting from charge-density wave (CDW) formation in $\text{Mo}_3\text{Al}_2\text{C}$. We carried out energy-band calculations for the β -Mn-type cubic cell on the basis of the full-potential linearized augmented-plane-wave (FLAPW) method. In the calculation, the energy bands split by the spin-orbit interaction due to the lack of inversion symmetry generate pairs of similar Fermi surfaces, i.e., small hole pockets from the 269th and the 270th bands, two hole surfaces from the 271st and the 272nd bands, and two electron surfaces from the 273rd and the 274th bands. Figure 6 clearly shows that the Fermi surfaces display a strong nesting along the wave vector $\mathbf{q} = (1,1,1)$ direction, which may cause electron-lattice instability in the cubic unit

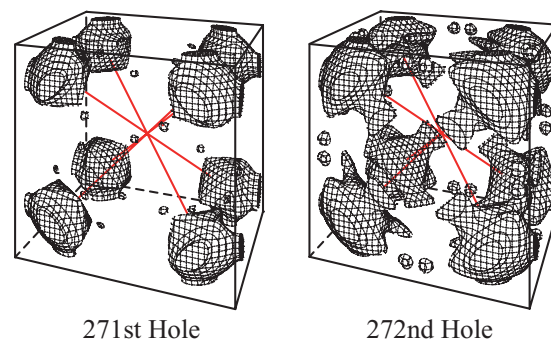


FIG. 6. (Color online) The hole Fermi surfaces consist of the 271st and the 272nd bands for $\text{Mo}_3\text{Al}_2\text{C}$. The red lines indicate the $[111]$ directions in the cubic Brillouin zone, along which the nesting vectors are likely oriented.

cell. Such a nesting property of Fermi surfaces can facilitate CDW formation.

In most cases, the CDW transition appears as an upturn in the resistivity $\rho(T)$. $\rho(T)$ of the present sample shows almost the same temperature dependence as that previously reported,⁶ the presence of an inflection point in $\rho(T)$ at ~ 150 K, which looks to be related to the transition. However, the samples including ours seem to be too inhomogeneous to exhibit an intrinsic anomaly in $\rho(T)$ owing to the inclusion of appreciable amounts of impurity phases and disorder.

The NMR spectrum exhibits a distinct change above 120 K. The broadening of and/or change in the NMR line shape owing to the CDW formation were observed in several compounds.^{11–13} With the onset of the CDW, the charge perturbation invokes spatial distribution of the EFG tensor at the observed nuclei. The significant change in the ^{27}Al NMR line shape in $\text{Mo}_3\text{Al}_2\text{C}$ can be ascribed to this effect. The phase transition is characterized by the peak of $1/T_2$. This phenomenon is associated with the sudden broadening of the NMR line. At the CDW transition, the modulation of the charge distribution and/or of atomic positions, which broadens the NMR central line, results in the distribution of local fields originating from nuclear dipoles. Consequently, $1/T_2$ is enhanced with decreasing temperature. Further increase in the distribution decouples the nuclear spin-spin interaction, resulting in a rapid decrease in $1/T_2$. Therefore, the peak of $1/T_2$ reflects the change in the nuclear dipolar field at

around CDW ordering. The origin behind the observation of the reduction in the density of states is not well understood at present. However, one possibility may be the formation of CDW, although a CDW-like anomaly has not been observed in previous resistivity measurements.^{5,6}

In conclusion, we discovered a phase transition in the normal state of noncentrosymmetric $\text{Mo}_3\text{Al}_2\text{C}$ using NMR and specific-heat measurements. A distinct peak of $1/T_2$, a sudden change in ^{27}Al NMR spectra, and an anomaly in the specific heat at ~ 130 K clearly indicate an abrupt change in the electronic state. In addition, the reduction in the conduction electron density below ~ 130 K is inferred from the decrease in both $1/(T_1T)$ and ^{27}K . Thus we conclude that the reduction in $D(E_F)$ is associated with the appearance of a gap on the Fermi surface, presumably resulting from a CDW transition. The decrease in $1/T_1$ in the superconducting state confirms that SC emerges in the ordered state with the partially quenched Fermi surface. This experimental finding must be taken into account to discuss the mechanism of SC in $\text{Mo}_3\text{Al}_2\text{C}$. Further investigation of the structural change and lattice softening of $\text{Mo}_3\text{Al}_2\text{C}$ can enable us to gain a better understanding of the transition.

We would like to thank Y. Ihara for valuable suggestions and comments. This work was partially supported by a Grant-in-Aid for Scientific Research on Priority Areas “Novel States of Matter Induced by Frustration” (19052003) and a Grant-in-Aid for Young Scientists (23740276).

*t-koyama@sci.u-hyogo.ac.jp

¹M. Hanawa, Y. Muraoka, T. Tayama, T. Sakakibara, J. Yamaura, and Z. Hiroi, *Phys. Rev. Lett.* **87**, 187001 (2001).

²T. Koyama, H. Yamashita, Y. Takahashi, T. Kohara, I. Watanabe, Y. Tabata, and H. Nakamura, *Phys. Rev. Lett.* **101**, 126404 (2008).

³J. Johnston, L. E. Toth, K. Kennedy, and E. R. Parker, *Solid State Commun.* **2**, 123 (1964).

⁴E. Bauer, G. Hilscher, H. Michor, Ch. Paul, E. W. Scheidt, A. Gribanov, Yu. Seropegin, H. Noël, M. Sigrist, and P. Rogl, *Phys. Rev. Lett.* **92**, 027003 (2004).

⁵E. Bauer, G. Rogl, Xing-Qiu Chen, R. T. Khan, H. Michor, G. Hilscher, E. Royanian, K. Kumagai, D. Z. Li, Y. Y. Li, R. Podloucky, and P. Rogl, *Phys. Rev. B* **82**, 064511 (2010).

⁶A. B. Karki, Y. M. Xiong, I. Vekhter, D. Browne, P. W. Adams, D. P. Young, K. R. Thomas, J. Y. Chan, H. Kim, and R. Prozorov, *Phys. Rev. B* **82**, 064512 (2010).

⁷I. Bonalde, H. Kim, R. Prozorov, C. Rojas, P. Rogl, and E. Bauer, *Phys. Rev. B* **84**, 134506 (2011).

⁸The signal from the impurity phase Mo_3Al_8 is not observed in the demonstrated data because the resonance conditions for $\text{Mo}_3\text{Al}_2\text{C}$ and impurity phases are completely different. Particularly, their $1/T_1$'s are different by several orders of magnitude, making the simultaneous observation of both signals difficult.

⁹Y. Kohori, Y. Noguchi, and T. Kohara, *J. Phys. Soc. Jpn.* **62**, 447 (1993).

¹⁰D. C. Johnston, *Phys. Rev. B* **74**, 184430 (2006).

¹¹P. Butaud, P. Ségransan, C. Berthier, J. Dumas, and C. Schlenker, *Phys. Rev. Lett.* **55**, 253 (1985).

¹²J. H. Ross Jr., Zhiyue Wang, and Charles P. Slichter, *Phys. Rev. B* **41**, 2722 (1990).

¹³S. Suh, W. G. Clark, P. Monceau, R. E. Thorne, and S. E. Brown, *Phys. Rev. Lett.* **101**, 136407 (2008), and references therein.